Available online at www.sciencedirect.com
ScienceDirect
Lithos 92 (2006) 576–587
LITHOS
www.elsevier.com/locate/lithos

Corundum+quartz and Mg-staurolite bearing granulite from the Limpopo Belt, southern Africa: Implications for a *P–T* path

Toshiaki Tsunogae [a,b,*], Dirk D. van Reenen [b]

[a] *Graduate School of Life and Environmental Sciences, University of Tsukuba, Ibaraki 305-8572, Japan*
[b] *Department of Geology, University of Johannesburg, P.O. Box 524, Auckland Park 2006, Republic of South Africa*

Received 31 May 2005; accepted 30 March 2006
Available online 12 June 2006

Abstract

A new occurrence of the rare corundum+quartz assemblage and magnesian staurolite has been found in a gedrite–garnet rock from the Central Zone of the Neoarchean Limpopo Belt in Zimbabwe. Poikiloblastic garnet in the sample contains numerous inclusions of corundum+quartz±sillimanite, magnesian staurolite+sapphirine±orthopyroxene, and sapphirine+sillimanite assemblages, as well as monophase inclusions. Corundum, often containing subhedral to rounded quartz, occurs as subhedral to euhedral inclusions in the garnet. Quartz and corundum occur in direct grain contact with no evidence of a reaction texture. The textures and Fe–Mg ratios of staurolite inclusions and the host garnet suggest a prograde dehydration reaction of St→Grt+Crn+Qtz+H_2O to give the corundum+quartz assemblage. Peak conditions of 890–930 °C at 9–10 kbar are obtained from orthopyroxene+sapphirine and garnet+staurolite assemblages. A clockwise *P–T* path is inferred, with peak conditions being followed by retrograde conditions of 4–6 kbar and 500–570 °C. The presence of unusually magnesian staurolite (Mg/[Fe+Mg]=0.47–0.53) and corundum+garnet assemblages provides evidence for early high-pressure metamorphism in the Central Zone, possibly close to eclogite facies. The prograde high-pressure event followed by high- to ultrahigh-temperature metamorphism and rapid uplifting of the Limpopo Belt could have occurred as a result of Neoarchean collisional orogeny involving the Zimbabwe and Kaapvaal Cratons.

Keywords: Corundum+quartz; Magnesian staurolite; Garnet+corundum; Granulite; Limpopo Belt; Southern Africa

1. Introduction

Since the first description of sapphirine+quartz assemblages from Antarctica by Dallwitz (1968), equilibrium mineral assemblages including sapphirine+quartz, spinel+quartz, and orthopyroxene+ sillimanite+quartz have been found in several granulite terranes, and are considered to represent evidence of extremely high-temperature conditions (e.g., *T*=900–1100 °C, *P*=7–13 kbar; see Harley, 1998, 2004 and references therein). These rocks, which form through ultrahigh-temperature (UHT) metamorphism, rarely contain corundum+quartz assemblages (e.g., Krogh, 1977; Powers and Bohlen, 1985; Lal et al., 1987; Perchuk et al., 1989; Motoyoshi et al., 1990; Guiraud et al., 1996; Shaw and Arima, 1998; Mouri et al., 2003, 2004). Although the textures of some corundum+quartz assemblages are apparently stable (e.g., Guiraud et al., 1996; Shaw and Arima, 1998; Mouri et al., 2003),

* Corresponding author. Tel.: +81 29 853 5239; fax: +81 29 851 9764.
E-mail address: tsunogae@arsia.geo.tsukuba.ac.jp (T. Tsunogae).

0024-4937/$ - see front matter © 2006 Elsevier B.V. All rights reserved.
doi:10.1016/j.lithos.2006.03.052

most published studies favour a metastable relationship involving corundum and quartz (e.g., Motoyoshi et al., 1990), in agreement with experimental studies suggesting that corundum and quartz should not coexist as a stable assemblage over the P–T range encountered in the crust and upper mantle (Harlov and Milke, 2002, 2004). However, Kawasaki (2005) reported the coexistence of corundum and quartz in experimental high-temperature (900 °C and 1200 °C at 8 kbar) studies of sedimentary rocks. Therefore, further study of the occurrence and relationship of natural corundum and quartz in a range of rocks is required in order to understand the implications of corundum + quartz assemblages.

This paper presents the first reported occurrence of a corundum + quartz assemblage in a gedrite–garnet rock from the Central Zone of the Limpopo Belt in Zimbabwe (Fig. 1). The rock also contains rare Mg-staurolite enclosed in poikiloblastic garnet. Although Fe–staurolite, a common mineral in amphibolite-facies pelitic rocks, is stable at $P<15$ kbar and $T=500$–700 °C in the KFASH system (Spear and Cheney, 1989), Mg-staurolite is an exceptionally rare mineral and is regarded to be stable under higher P–T conditions (e.g., Fockenberg, 1998). The present results have important implications with respect to the occurrence of corundum + quartz assemblages and Mg-staurolite in granulite-facies rocks formed by Archean continental collision orogeny.

2. General geology

The Limpopo Belt of southern Africa is a classic example of a high-grade metamorphic terrane situated between two Archean Cratons: the Zimbabwe Craton in the north and the Kaapvaal Craton in the south (Fig. 1) (e.g., van Reenen et al., 1987, 1990; Rollinson and Blenkinsop, 1995). The belt has been subdivided into three zones based on structural patterns and lithologies: the Central Zone (CZ), the Southern Marginal Zone (SMZ), and the Northern Marginal Zone (NMZ). The CZ is characterized by the presence of pure metaquartzite, marble, and calc-silicate rocks, and the widespread occurrence of leucocratic gneisses. Available age data for the NMZ and SMZ suggest a single high-grade metamorphic event that occurred between 2.6 and 2.7 Ga (e.g., Barton and van Reenen, 1992; Berger et al., 1995; Kreissig et al., 2001). The CZ has been affected by a thermal event of ca. 2.0 Ga after the 2.6–2.7 Ga event (e.g., Kamber et al., 1995; Jaeckel et al., 1997; Holzer et al., 1998; Kröner et al., 1999), probably reflecting a stage of deformation and anatexis (McCourt and Armstrong, 1998).

Several of the P–T paths proposed for the CZ are characterized by peak metamorphism of 800–900 °C at

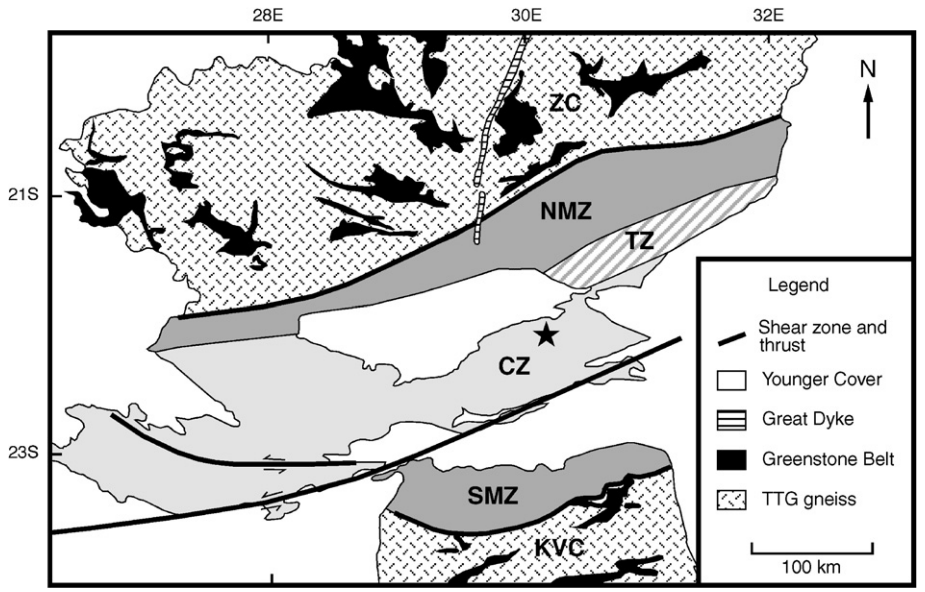

Fig. 1. Simplified geological map of the Limpopo Belt (after Rollinson and Blenkinsop, 1995) and adjacent areas showing the locality of the sample (star) discussed in this study. NMZ: Northern Marginal Zone, CZ: Central Zone, SMZ: Southern Marginal Zone, TZ: Transition Zone, ZC: Zimbabwe Craton, KVC: Kaapvaal Craton.

7–9 kbar followed by near isothermal decompression to 4–5 kbar along a clockwise *P–T* path (Windley et al., 1984; Droop, 1989; Tsunogae and Miyano, 1989). In contrast, Perchuk et al. (2000), van Reenen et al. (2004), and Zeh et al. (2004) suggested retrograde decompression–cooling paths for the CZ.

3. Petrography

The gedrite–garnet rock (sample MPL867) examined in this study was collected by Malcohm Light from the Beit Bridge Complex in the CZ north of Beitbridge in Zimbabwe (Fig. 1). The sample is composed of gedrite (30–40%), garnet (15–20%), quartz (20–30%), orthopyroxene (10–15%), cordierite (2–5%), and sillimanite (1–2%). The rock is characterized by the presence of poikiloblastic garnet (1–6 mm in length) in the matrix of gedrite, orthopyroxene, and quartz (Fig. 2a). The garnet contains numerous inclusions of quartz, sapphirine, staurolite, sillimanite, corundum, rutile, and gedrite (Fig. 3a). The inclusion minerals exhibit a complex host–inclusion relationship. Corundum (0.1–1.1 mm), often containing subhedral to rounded quartz, occurs as subhedral to euhedral inclusions in the garnet (Fig. 2a). Quartz and corundum occur in direct grain contact with no evidence of a reaction texture (Fig. 3b). Such host corundum vs. inclusion quartz relationships are rare but have been reported (e.g., Mouri et al., 2003), although the two minerals are commonly separated by later sillimanite. Sapphirine inclusions (0.1–1.2 mm) in garnet are pale blue and mostly irregular in shape (Fig. 3c), but rare euhedral grains are also present (Fig. 2b). Sapphirine also contains staurolite (<100 μm) and rare orthopyroxene (<20 μm) in the same grain (Fig. 3c), while sillimanite (<30 μm) if present is not accompanied by staurolite or orthopyroxene (Fig. 3d). Staurolite also occurs in garnet directly without sapphirine (Fig. 2b).

Poikiloblastic garnet is occasionally mantled by a corona of fine-grained cordierite with or without orthopyroxene (Fig. 2a). Sillimanite adjacent to gedrite is commonly surrounded by symplectitic sapphirine, spinel, and cordierite (Fig. 2c).

Matrix gedrite is medium-grained (0.2–0.4 mm) and forms aggregates of up to 3 cm in length (Fig. 2d). Coarse-grained (up to 5 mm) poikiloblastic orthopyroxene with inclusions of gedrite and quartz

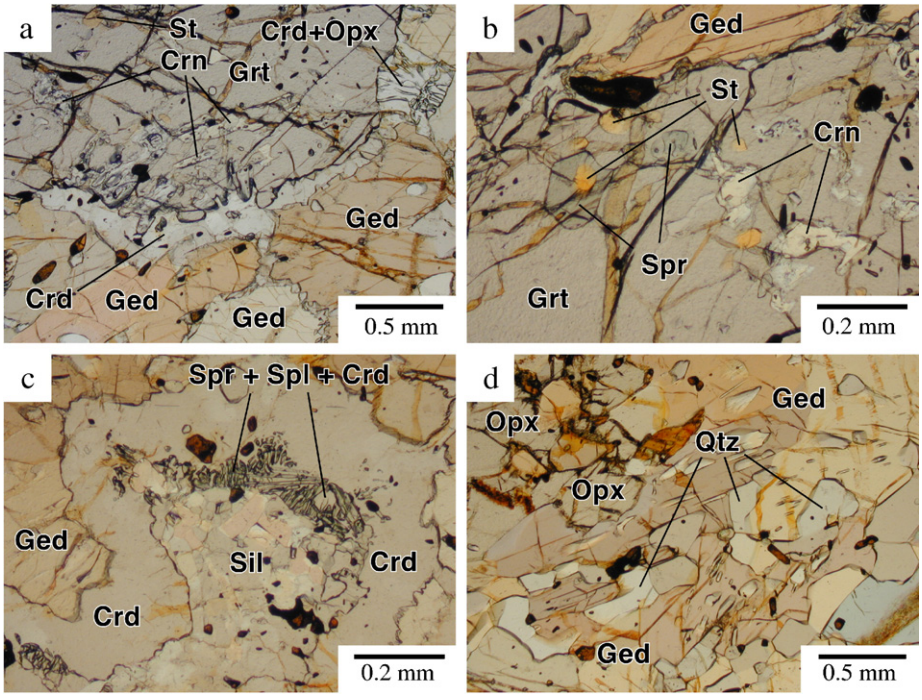

Fig. 2. Photomicrographs of the studied gedrite–garnet rock (sample MPL867). (a) Porphyroblastic garnet in a matrix of gedrite. The garnet contains inclusions of corundum and staurolite, and is rimmed by a corona of cordierite and orthopyroxene. (b) Corundum, staurolite, and sapphirine inclusions in garnet. Staurolite is occasionally included in sapphirine. (c) Sapphirine+spinel+cordierite corona developed between sillimanite and gedrite. (d) Intergrowth of poikiloblastic orthopyroxene and gedrite. Mineral abbreviations are after Kretz (1983).

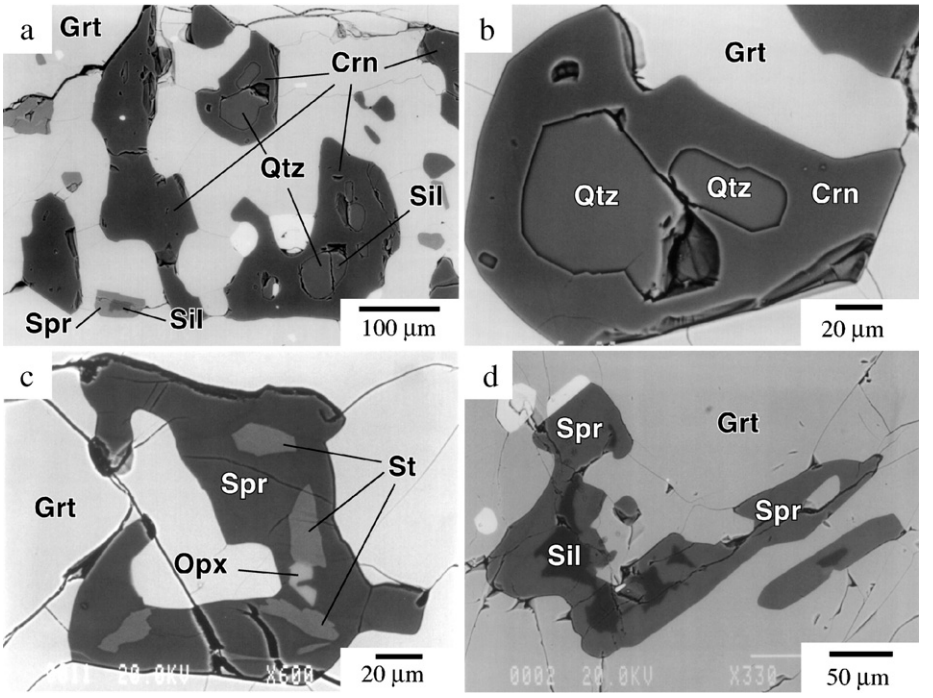

Fig. 3. Back-scattered electron images showing detailed textures in sample MPL867. (a) Apparently equilibrium corundum+quartz assemblage enclosed in garnet. Sapphirine and quartz contain rare inclusions of sillimanite. (b) Corundum+quartz assemblage with no reaction texture between them. (c) Irregular-shaped sapphirine inclusion in garnet. The sapphirine contains inclusions of staurolite and orthopyroxene. (d) Irregular sillimanite surrounded by sapphirine.

coexists with gedrite in garnet-absent portions of the rock (Fig. 2d).

4. Mineral chemistry

Chemical analyses of minerals were performed using an electron microprobe analyzer (JXA8621, JEOL) at the University of Tsukuba. Analyses were performed under conditions of 20 kV accelerating voltage and 10 nA sample current, and data were regressed using an oxide-ZAF correction program supplied by JEOL. Representative compositions of minerals in the analyzed sample are given in Table 1. The Fe^{3+} content of sapphirine was calculated by the method of Higgins et al. (1979). Mineral compositions are shown in Figs. 4–8. The X_{Mg} [Mg/(Fe+Mg)] ratios for the relevant phases decrease in the order cordierite (0.89–0.91)> sapphirine (0.80–0.84)>gedrite (0.70–0.79)≈orthopyroxene (0.71–0.77)>spinel (0.45–0.48)>staurolite (0.43–0.53)≈garnet (0.44–0.52).

Garnet is present essentially as a solid solution between pyrope and almandine (X_{Mg}=0.44–0.52) with minor grossular (<5 mol.%) and spessartine (<1 mol.%). Both the core and rim of the analyzed garnet grains are rich in Mg and are nearly compositionally homogeneous ($Alm_{46–49}Pyr_{48–50}Grs_{3–4}Sps_{0–1}$). The garnet rim adjacent to gedrite and cordierite is slightly enriched in Fe ($Alm_{50–54}Pyr_{42–45}Grs_{3–4}Sps_{0–1}$).

Sapphirine is Mg-rich (X_{Mg}=0.80–0.84) with an (Mg, Fe)O:Al_2O_3:SiO_2 ratio close to the representative 7:9:3 composition (Fig. 4). The calculated $Fe^{3+}/(Fe^{2+}+Fe^{3+})$ ratio is generally low (0.01–0.16). Sapphirine enclosed in garnet is relatively Si-rich (Si=1.48–1.55 pfu) in comparison to the symplectitic phase (1.36–1.39). Other components total less than 0.2 wt.%.

Spinel is present as a solid solution between hercynite and Mg-spinel (X_{Mg}=0.45–0.48) with very minor MnO (0.1–0.6 wt.%), Cr_2O_3 (0.19–0.42 wt.%), and ZnO (0.38–0.52). The calculated $Fe^{3+}/(Fe^{2+}+Fe^{3+})$ ratio indicates that all Fe in the spinel is Fe^{2+}.

The composition of staurolite in the sample is shown in Fig. 5 for comparison with available data for staurolite inclusions in garnet from other granulite terranes. The present staurolite is unusually Mg-rich (X_{Mg}=0.43–0.53) and contains up to 1.4 wt.% TiO_2. Staurolite found as inclusions in garnet (without

Table 1
Representative electron microprobe analyses of minerals in sample MPL867

Minerals	Grt core	Grt1 rim	St in Grt	St in Spr	Spr2 in Grt	Spr3 in Grt	Spr4 with Crd	Spl4 with Crd	Crd4 with Grt	Crn in Grt	Opx in Spr	Opx with Ged	Opx4 with Crd	Ged core	Ged with Opx
O*	12	12	46	46	20	20	20	4	18	3	6	6	6	23	23
SiO_2	40.33	40.22	26.34	27.23	12.79	12.82	11.41	0.05	48.93	0.02	51.14	51.42	52.03	44.63	46.60
Al_2O_3	23.10	22.81	57.03	54.49	62.52	63.37	65.63	63.72	33.52	99.45	7.06	5.91	4.19	17.12	14.74
TiO_2	0.05	0.01	1.10	1.25	0.03	0.06	0.06	0.05	0.22	0.05	0.11	0.10	0.11	0.60	0.51
Cr_2O_3	0.00	0.01	0.19	0.07	0.10	0.13	0.05	0.29	0.03	0.03	0.05	0.03	0.01	0.02	0.00
Fe_2O_3										0.24					
FeO	21.58	24.52	7.88	9.14	6.67	6.23	7.10	23.97	2.07		14.14	16.43	17.84	12.50	13.00
MnO	0.12	0.16	0.03	0.01	0.00	0.00	0.00	0.01	0.02	0.00	0.01	0.04	0.02	0.02	0.06
MgO	13.26	11.03	5.00	4.49	16.90	16.62	15.31	11.12	12.19	0.02	26.12	25.53	25.13	19.47	19.44
ZnO	0.04	0.01	0.13	0.09	0.00	0.00	0.01	0.52	0.00	0.00	0.05	0.00	0.00	0.00	0.00
CaO	1.26	1.40	0.00	0.00	0.01	0.02	0.00	0.00	0.01	0.02	0.05	0.08	0.09	0.49	0.47
Na_2O	0.00	0.03	0.00	0.00	0.00	0.01	0.00	0.01	0.06	0.00	0.00	0.03	0.01	1.41	1.23
K_2O	0.00	0.01	0.00	0.00	0.00	0.01	0.00	0.00	0.00	0.01	0.01	0.00	0.00	0.02	0.00
Total	99.74	100.20	97.69	96.77	99.02	99.26	99.58	99.75	97.05	99.84	98.75	99.58	99.43	96.28	96.04
Si	3.009	3.028	7.149	7.494	1.532	1.527	1.361	0.001	4.963	0.000	1.850	1.865	1.902	6.344	6.633
Al	2.031	2.024	18.236	17.672	8.822	8.896	9.222	2.000	4.006	1.994	0.301	0.253	0.181	2.867	2.472
Ti	0.003	0.001	0.224	0.258	0.003	0.005	0.005	0.001	0.017	0.001	0.003	0.003	0.003	0.064	0.054
Cr	0.000	0.000	0.040	0.015	0.009	0.012	0.005	0.006	0.002	0.000	0.001	0.001	0.000	0.002	0.000
Fe^{3+}					0.104	0.038	0.053	0.000		0.003					
Fe^{2+}	1.346	1.544	1.787	2.103	0.563	0.583	0.655	0.534	0.176	0.000	0.428	0.498	0.545	1.485	1.547
Mn	0.008	0.010	0.006	0.001	0.000	0.000	0.000	0.000	0.001	0.000	0.000	0.001	0.000	0.003	0.007
Mg	1.473	1.236	2.020	1.842	3.014	2.949	2.719	0.441	1.843	0.000	1.408	1.380	1.368	4.122	4.121
Zn	0.002	0.000	0.026	0.019	0.000	0.000	0.001	0.010	0.000	0.000	0.001	0.000	0.000	0.000	0.000
Ca	0.101	0.112	0.000	0.000	0.001	0.002	0.001	0.000	0.001	0.000	0.002	0.003	0.003	0.075	0.072
Na	0.000	0.004	0.000	0.000	0.000	0.001	0.000	0.000	0.012	0.000	0.000	0.002	0.001	0.388	0.338
K	0.000	0.001	0.000	0.000	0.000	0.002	0.000	0.000	0.000	0.000	0.001	0.000	0.000	0.004	0.000
Total	7.973	7.961	29.489	29.404	14.050	14.015	14.021	2.995	11.022	2.000	3.996	4.006	4.005	15.354	15.246
Mg/(Fe+Mg)	0.52	0.44	0.53	0.47	0.82	0.83	0.79	0.45	0.91	1.00	0.77	0.73	0.72	0.74	0.73

*Number of oxygen.
1 in contact with Crd, 2 including Sil, 3 including St and Opx, 4 retrograde mineral.

sapphirine) is more Mg-rich (X_{Mg}=0.47–0.53) than that occurring in sapphirine (0.43–0.47). Other components such as Cr_2O_3 and ZnO are minor and total less than 0.3 wt.%. As shown in Fig. 5a, the staurolite data exhibit a consistent substitution of $AlTi \leftrightarrow SiR^{2+}$ (e.g., Hiroi et al., 1994).

The orthopyroxene composition varies according to the mode of occurrence (Fig. 6). Three modes are observed. Orthopyroxene in sapphirine exhibits the highest X_{Mg} ratio (0.76–0.77) and Al_2O_3 content (7.0–7.1 wt.%), followed by coarse-grained porphyroblastic orthopyroxene (0.73–0.74, 5.8–5.9 wt.%), and symplectitic orthopyroxene (0.71–0.72, 4.1–4.2 wt.%).

Gedrite is magnesian (X_{Mg}=0.70–0.79) and characterized by a high Al_2O_3 content (14.8–17.5 wt.%). Coarse-grained matrix gedrite associated with garnet exhibits the highest Na content, up to 0.47 pfu (1.7 wt.% Na_2O). Such Na-rich gedrite has been reported for UHT rocks from southern India (e.g., Koshimoto et al., 2004; Shimpo et al., 2006). As shown in Fig. 7a, $Na+Al^{IV}$ increases linearly with decreasing Si, reflecting the substitution of $NaAl^{IV} \leftrightarrow Si$. Compositional zoning within single coarse-grained gedrite crystal is absent. Fine-grained gedrite inclusions in garnet display the highest Al_2O_3 content (17.4–17.6 wt.%) and X_{Mg} (0.75–0.79), while gedrite associated with orthopyroxene exhibits the lowest Na_2O content (1.2–1.3 wt.%).

Corundum in the present sample is close to the ideal chemistry (Al_2O_3). Previous reports on corundum+quartz assemblages have suggested that a small amount of Fe^{3+} and Cr^{3+} may replace Al^{3+}. Guiraud et al. (1996) obtained ~0.73 wt.% Fe_2O_3 in corundum associated with magnetite, and a similar Fe_2O_3 content of ~0.74 wt.% was found for corundum in a magnetite-free pelitic granulite from the Eastern Ghats (Shaw and Arima, 1998). Corundum from Namaqualand exhibits a considerably higher Fe_2O_3 content of 0.68–1.4 wt.% (Mouri et al., 2003), while Motoyoshi et al. (1990) reported up to 0.4 wt.% Cr_2O_3

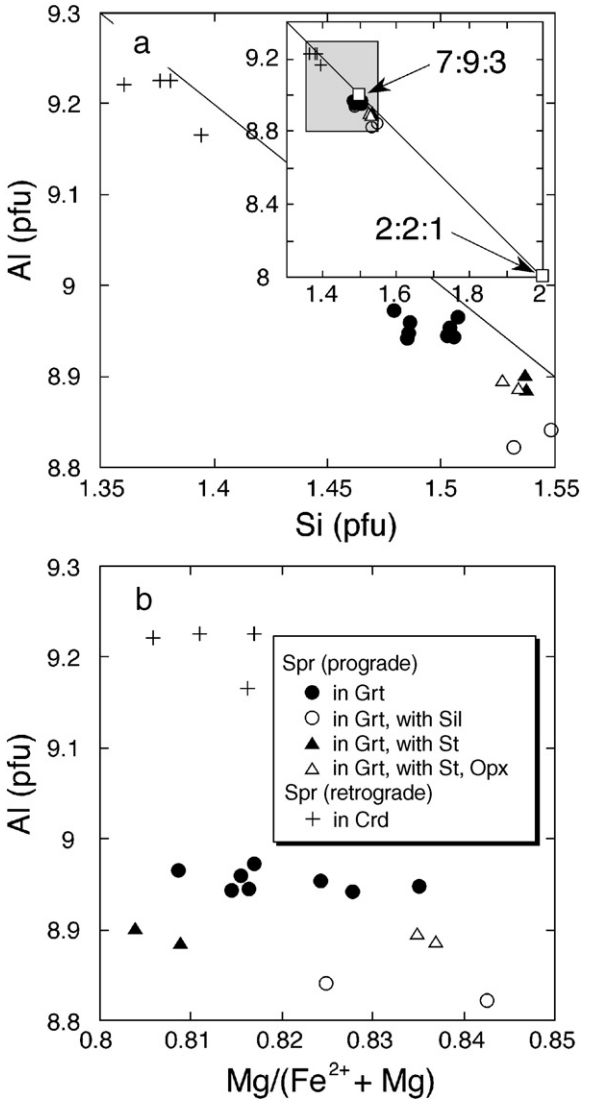

Fig. 4. (a) Al versus Si (pfu) diagram showing compositional variations of sapphirine in terms of Al and Si. Squares with labels 7:9:3 and 2:2:1 in the figure imply representative compositions of $Mg_{1.75}Al_{4.5}Si_{0.75}O_{10}$ and $Mg_2Al_4SiO_{10}$, respectively. (b) $Mg/(Fe^{2+}+Mg)$ versus Al (pfu) diagram showing the variation of sapphirine compositions depending on their mode of occurrence.

and 0.68 wt.% Fe_2O_3 in corundum occurring between spinel and quartz. Corundum in the present sample exhibits lower Fe_2O_3 and Cr_2O_3 than these previous reports, 0.16–0.32 and 0.03–0.10 wt.%, respectively.

Cordierite in the sample has a uniform magnesian composition of X_{Mg}=0.89–0.91, and no compositional changes are seen in relation to coexisting minerals. The compositions of sillimanite (Al_2SiO_5), quartz (SiO_2), and rutile (TiO_2) are close to the ideal chemistry, although sillimanite contains small amounts of Fe_2O_3 (0.14–1.1 wt.%).

5. Metamorphic reactions

The textures described in the sample can be divided into three major stages (prograde, near-peak, and retrograde) based on host–inclusion relationships, grain shape, and size. These textures are discussed here in reference to the FeO–MgO–Al_2O_3–SiO_2(–H_2O) [FMAS(H)] system. The compositions and assemblages of minerals in these three stages are shown on SiO_2–(FeO+MgO)–Al_2O_3 and Al_2O_3–FeO–MgO diagrams in Fig. 8.

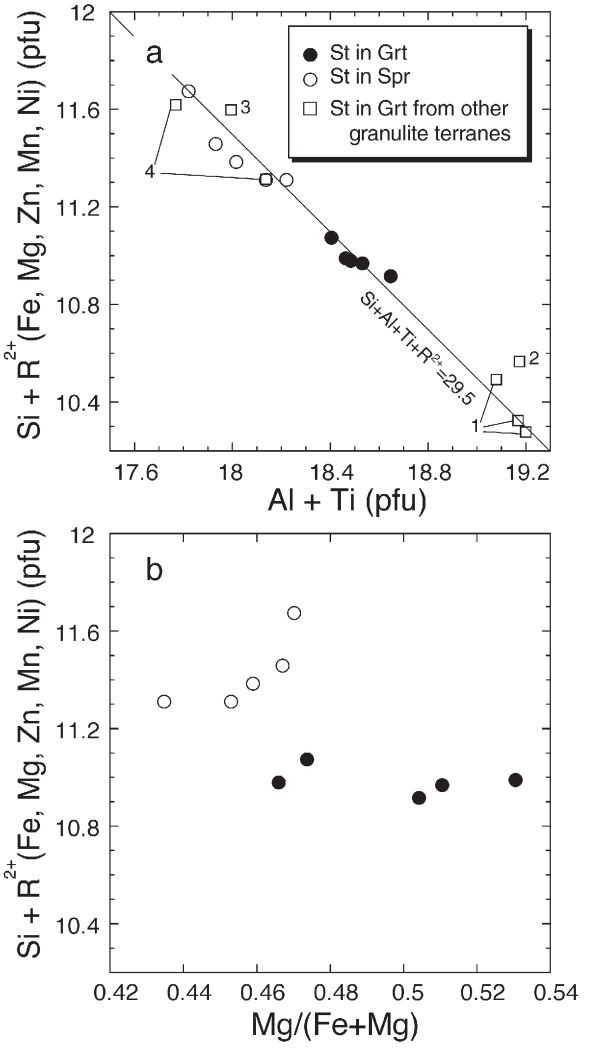

Fig. 5. Compositional diagrams showing staurolite chemistry. (a) Al+Ti versus $Si+R^{2+}$ (Fe, Mg, Zn, Mn, Ni) diagram. Available staurolite compositions from granulite-facies terranes are also shown. 1: Hiroi et al. (1994); 2: Droop and Bucher-Nurminen (1984); 3: Schreyer et al. (1984); 4: Osanai et al. (1992). (b) Mg/(Fe+Mg) versus $Si+R^{2+}$ diagram showing the different Mg/(Fe+Mg) ratios of staurolite depending on textures.

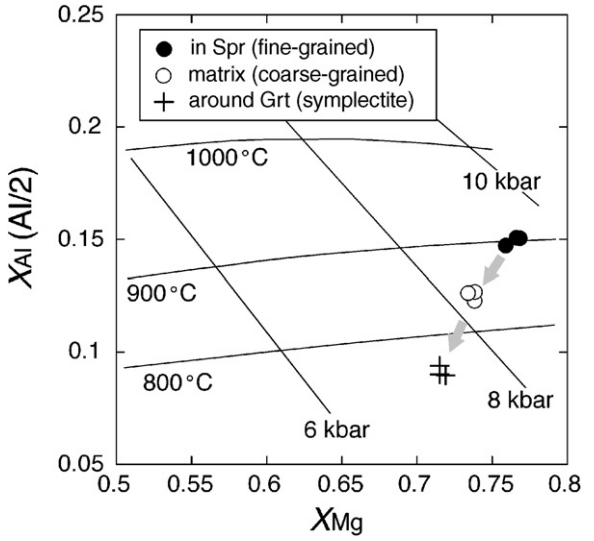

Fig. 6. Compositional diagram showing orthopyroxene chemistry. *P–T* grids are after Hensen and Harley (1990). Arrays indicate a *P–T* path discussed in the text. Orthopyroxene in the sample exhibits three different occurrences: fine-grained prograde phase in sapphirine, coarse-grained matrix phase with quartz and gedrite, and retrograde phase with cordierite around garnet.

5.1. Prograde reactions

Prograde reactions are reflected by the occurrence of inclusions in porphyroblastic minerals. Mg-rich staurolite is included in both sapphirine and garnet, suggesting formation as a result of the following continuous reaction in the FMASH system (Figs. 8a and d):

$$\mathrm{St} \rightarrow \mathrm{Grt} + \mathrm{Spr} + \mathrm{Sil/Ky} + \mathrm{H_2O} \quad (1)$$

It should be noted, however, that this reaction is not balanced, since X_{Mg} of the reactant staurolite (0.43–0.47) is lower than that of the product minerals (0.49–0.52 for garnet, 0.80–0.84 for sapphirine). It is thus inferred that the staurolite must have been more Mg-rich ($X_{Mg}>0.47$) prior to the formation of garnet and sapphirine.

Staurolite inclusions in garnet without sapphirine exhibit X_{Mg} ratios (0.47–0.53) similar to that of the host garnet (0.49–0.52) (Fig. 8d). This suggests that the corundum+quartz assemblage in the garnet is formed by the following FMASH continuous reaction:

$$\mathrm{St} \rightarrow \mathrm{Grt} + \mathrm{Crn} + \mathrm{Qtz} + \mathrm{H_2O} \quad (2)$$

Reaction (2) is considered to have contributed to the formation of the garnet–corundum–quartz association in the sampled rock (Fig. 3b). The presence of fine-grained rutile inclusions in garnet, probably derived from TiO_2 in staurolite, also supports the progress of reactions (1) and (2).

5.2. Near-peak assemblages

The mineral assemblages present at peak metamorphism are inferred from the coarse-grained matrix minerals: quartz, garnet, gedrite, and orthopyroxene (or sillimanite) (Figs. 8b and e). Garnet and sillimanite define aluminous domains in the rock, surrounded by orthopyroxene, gedrite, and quartz. Sillimanite and orthopyroxene display no direct contact relationship,

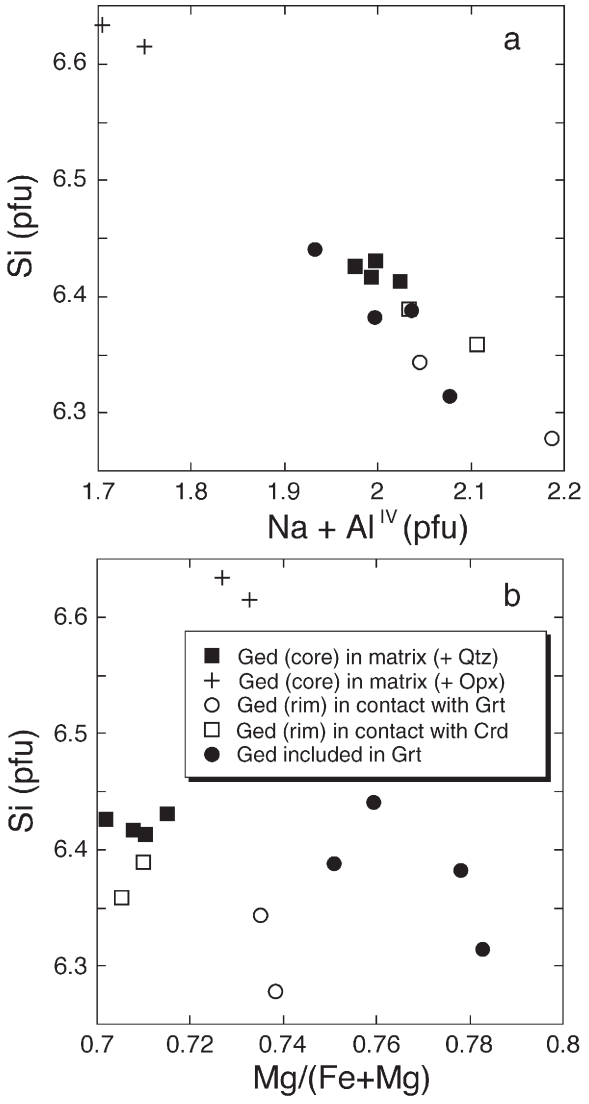

Fig. 7. Compositional diagrams showing gedrite chemistry. (a) Na+Al^{IV} versus Si diagram. (b) Mg/(Fe+Mg) versus Si diagram showing the different Mg/(Fe+Mg) ratios of gedrite depending on coexisting minerals.

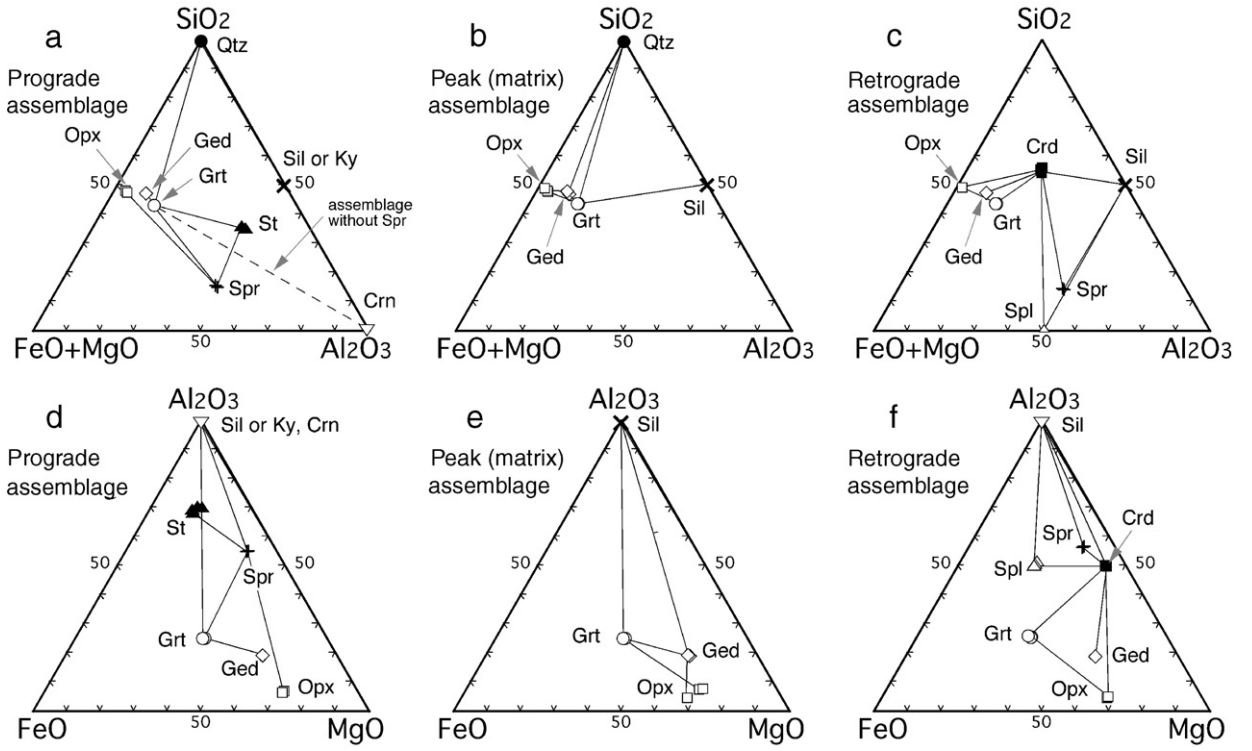

Fig. 8. Triangular diagrams showing mineral assemblages and chemistry for sample MPL867. (a) to (c) are SiO_2–(FeO+MgO)–Al_2O_3 diagrams, and (d) to (f) are Al_2O_3–FeO–MgO diagrams. (a and d) Prograde mineral assemblages occurring as inclusions in garnet. (b and e) Near-peak mineral assemblages in the matrix. (c and f) Retrograde mineral assemblages forming coronas around garnet and sillimanite. The equilibrium mineral assemblages are presented by tie lines.

whereas gedrite and quartz are occasionally found with granoblastic textures.

5.3. Retrograde reactions

Retrograde reactions are observed as corona and symplectite textures around early coarse-grained minerals. A common example is the corona of cordierite+orthopyroxene found to mantle some garnets (Figs. 2a, 8c and f). This occurrence suggests the following FMAS continuous reaction:

$$\mathrm{Grt} + \mathrm{Qtz} \rightarrow \mathrm{Crd} + \mathrm{Opx} \quad (3)$$

The progress of reaction (3) is supported by the decreasing Mg content in garnet from the core to the rim. A corona texture of sapphirine+cordierite and spinel+cordierite between sillimanite and gedrite (Figs. 2b, 8c and f) suggests the following FMASH reaction:

$$\mathrm{Ged} + \mathrm{Sil} \rightarrow \mathrm{Spr/Spl} + \mathrm{Crd} + \mathrm{H_2O} \quad (4)$$

Although the above reaction is written as a dehydration reaction, it is suggested that cordierite would have incorporated the H_2O liberated by gedrite, thus conserving water. Reaction (4) could have occurred during retrograde metamorphism (e.g., Goscombe, 1992), probably at the same stage as reaction (3).

6. Metamorphic *P–T* conditions

Temperatures close to the peak metamorphism were estimated based on sapphirine–orthopyroxene, garnet-staurolite and Al-in-orthopyroxene geothermometers applied to inclusion minerals in poikiloblastic garnet. Geothermobarometers including cordierite were adopted to obtain retrograde conditions. Errors in calculated *P–T* results as discussed in individual methods are regarded to be approximately ±100 °C and ±2 kbar.

6.1. Sapphirine–orthopyroxene geothermometer

Kawasaki and Sato (2002) formulated this geothermometer experimentally for application to UHT rocks using natural mineral pairs. Application of the method to

orthopyroxene inclusions and host sapphirine yields a temperature range of 890–930 °C.

6.2. Garnet-staurolite geothermometer

The experimentally determined Fe–Mg exchange between synthetic garnet and staurolite (Koch-Müller, 1997) was applied to fine-grained staurolite and adjacent garnet, yielding a temperature range of 900–920 °C, similar to the range calculated for sapphirine + orthopyroxene.

6.3. Al-solubility in orthopyroxene

Fig. 6 shows an X_{Mg} vs. X_{Al} plot for the three types of orthopyroxene present in the sample. Based on the isotherms and isobars derived from the theoretical study by Hensen and Harley (1990), prograde fine-grained orthopyroxene included in sapphirine equilibrates under *P–T* conditions of ca. 900 °C and 9–10 kbar. Slightly lower conditions were obtained for matrix orthopyroxene (800–850 °C and 8–9 kbar) and symplectitic orthopyroxene with cordierite (<800 °C and 7–8 kbar).

6.4. Garnet–cordierite geothermobarometers

The rim compositions of garnet and corona cordierite yield much lower temperatures than the other geothermometers. For example, the experimental methods of Perchuk and Lavrent'eva (1983) and Nichols et al. (1992), applicable to rim and corona compositions, give temperatures of 500–520 °C and 550–570 °C, respectively, at 4 kbar. This assemblage was also adopted for pressure estimates based on the garnet–cordierite–sillimanite–quartz geobarometer. The experimental calibration of Aranovich and Podlesskii (1989) gives a pressure range of 4.2–6.2 kbar at 600 °C. These results suggest retrograde *P–T* conditions of 4–6 kbar and 500–570 °C.

7. Discussion

7.1. Corundum + quartz from the Limpopo Belt

Corundum + quartz assemblages in apparent textural equilibrium occur as inclusions in garnet within the gedrite–garnet rock from the CZ of the Limpopo Belt. Summarizing published occurrences of corundum and quartz, Harlov and Milke (2002) proposed the following possible relationships: (i) different assemblages are juxtaposed during later deformation, (ii) corundum may be a partial melt restite brought into arbitrary contact with quartz, which crystallized later from the associated melt, (iii) corundum is formed by later exsolution from spinel associated with quartz, and (iv) corundum is a reaction product generated in the presence of quartz. A very careful examination of the present sample leads to the conclusion that none of these models is appropriate for this corundum + quartz assemblage, since (i) there is no evidence for superimposed deformation, (ii) corundum includes quartz, and thus cannot be restitic, (iii) spinel or magnetite is not associated with corundum and quartz, and (iv) reaction (2) suggests that corundum and quartz formed at the same stage from staurolite. It is thus concluded that the occurrence of corundum + quartz in sample MPL867 is unique among the occurrences reported to date.

Harlov and Milke (2002) conducted an experimental investigation of the stability of corundum + quartz and concluded that the assemblage is metastable based on the growth of kyanite in the stability field of sillimanite along grain boundaries between these two minerals. However, Kawasaki (2005) confirmed the coexistence of corundum and quartz at high temperature (900 °C and 1200 °C at 8 kbar) based on experimental studies of sedimentary rocks. The question as to whether corundum + quartz can form a stable mineral assemblage, and the possible stability field for this assemblage, therefore remains open for debate, suggesting that further experimental and thermodynamic investigations of this assemblage are necessary.

7.2. Implications for a P–T path

The presence of unusual Mg-rich staurolite (X_{Mg} = 0.47–0.52) as inclusion in garnet is regarded as evidence for high-pressure prograde metamorphism in the CZ. Schreyer et al. (1984) reported similar Mg-rich staurolite ($X_{Mg} \approx 0.51$) from the CZ in South Africa, but did not consider the possibility of such high-pressure metamorphism. According to the experimental results of Schreyer (1988), pure Mg-staurolite is stable in the MASH system at $P > 14$ kbar and $T > 710$–760 °C. Fockenberg (1998) re-investigated staurolite stability and obtained high-*P–T* conditions of 12–66 kbar and 608–918 °C (Fig. 9). Peacock and Goodge (1995) reported relic staurolite inclusions ($X_{Mg} = 0.58$) in almandine–pyrope garnet in a retrogressed eclogite from the Miller Range, Antarctica, which display peak pressure conditions of $P = 12$–16 kbar. Staurolite with a highly magnesian composition ($X_{Mg} = 0.74$–0.78) has also been found in retrogressed eclogite and garnet–corundum rocks from the Donghai District of China (Enami and Zang, 1988). Significantly, magnesian

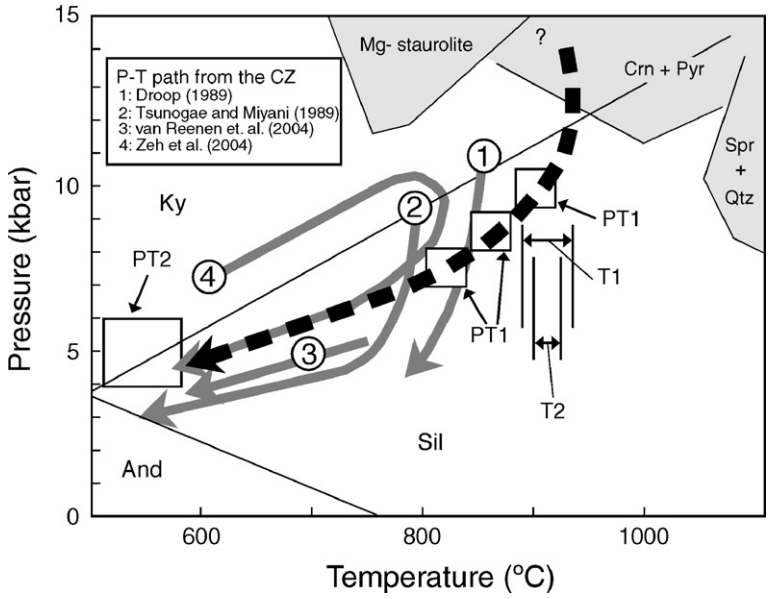

Fig. 9. *P–T* diagrams showing a *P–T* trajectory constructed for mineral assemblages in sample MPL867 (dashed array). Some published *P–T* paths from the CZ are also shown (paths 1 to 4). The stability field of Mg-staurolite was taken from Fockenberg (1998) and that of sapphirine+quartz from Hensen and Harley (1990) and Harley (1998). Phase relations of alumino silicates are based on thermodynamic data of Helgeson et al. (1978). The stability of corundum+garnet was taken from Shimpo et al. (2006). Pressure and temperature ranges in the figure are calculated using the following methods: T1: sapphirine–orthopyroxene geothermometer, T2: garnet-staurolite geothermometer, PT1: Al solubility in orthopyroxene geothermobarometers (Fig. 6), PT2: garnet–cordierite–sillimanite–quartz geothermobarometers.

staurolite (X_{Mg}=0.53–0.57) synthesized experimentally by Hellman and Green (1979) at P=24–26 kbar and T=740–760 °C has a composition close to that of the present staurolite (X_{Mg}=0.47–0.53). The available experimental and petrological studies thus indicate that the staurolite from the examined sample may have formed at high pressure.

Further evidence for a high-pressure event in the CZ is suggested by the presence of corundum and garnet in the sample. The stability field of corundum+garnet without orthopyroxene is not well constrained, and previous reports of equilibrium corundum–garnet assemblages have largely been derived for eclogites (e.g., Enami and Zang, 1988) and mantle-derived rocks (e.g., Kornprobst et al., 1990). A pyroxene-free corundum+garnet assemblage has been found in ultrahigh-pressure terranes (e.g., Zhang et al., 2004) and high-pressure granulites (e.g., Grew, 1986; Shimpo et al., 2006). The available petrological data suggest that the corundum+garnet assemblage is stable to pressures greater than 12 kbar (Shimpo et al., 2006). Although rare, several previous studies have reported on corundum in garnet-bearing rocks in the CZ of the Limpopo Belt (e.g., Horrocks, 1983; Droop, 1989). The occurrence of the rare corundum+garnet assemblage in more than one locality in the CZ might suggest that the area underwent a regional high-pressure event. Previous reports on relic kyanite in pelitic granulite from the CZ (e.g., Tsunogae and Miyano, 1989; Zeh et al., 2004) are consistent with the present model of high-pressure prograde metamorphism. The gedrite–garnet rock subsequently underwent a high to UHT peak event (T=890–930 °C at P=9–10 kbar; Fig. 9), probably during exhumation. The presence of retrograde symplectite textures suggests that the CZ has been exhumed from deep to mid-crustal levels. The final retrograde *P–T* conditions of 4 kbar and 500–570 °C are consistent with the results from previous studies (e.g., Perchuk et al., 2000; van Reenen et al., 2004; Zeh et al., 2004).

The metamorphic *P–T* path inferred from the new petrological data presented here supports a single clockwise *P–T* trajectory for the CZ, consistent with previous results (Fig. 9). However, this paper provides the first evidence in favour of a high-pressure stage possibly close to eclogite-facies conditions based on the presence of Mg-rich staurolite and corundum+garnet. The high-pressure metamorphism and subsequent high- to UHT event proposed in this study have important implications for the tectonic evolution of the Limpopo high-grade metamorphism, which is regarded to have resulted from the collision of two Archean Cratons (Roering et al., 1992).

Acknowledgements

We thank Dr. N. Nishida for his assistance with microprobe analyses and Dr. Y. Kaneko for thermodynamic calculations. The first author thanks the Geology Department of the University of Johannesburg for facilities and support. Partial funding for this project was supported by a Grant-in-Aid for Scientific Research (B) from the Japanese Ministry of Education, Culture, Sports, Science and Technology (MEXT) to TT (No. 17340158). DDVR acknowledges an NRF grant and financial support from the University of Johannesburg. Dr. Daniel E. Harlov, Dr. Hassina Mouri, and Prof. Christian Nicollet provided helpful comments that aided in improving our presentation. We thank these referees as well as Dr. Sajeev K. for his editorial comments.

References

Aranovich, L.Y., Podlesskii, K.K., 1989. Geothermobarometry of high-grade metapelites: simultaneously operating reactions. Spec. Publ. - Geol. Soc. Lond. 43, 45–61.

Barton Jr., J.M., van Reenen, D.D., 1992. When was the Limpopo Orogeny? Precambrian Res. 55, 7–16.

Berger, M., Kramers, J.D., Nägler, F.T., 1995. Geochemistry and geochronology of charnoenderbites in the Northern Marginal Zone of the Limpopo Belt, southern Africa, and genetic models. Schweiz. Mineral. Petrogr. Mitt. 75, 17–42.

Dallwitz, W.B., 1968. Co-existing sapphirine and quartz in granulite from Enderby Land, Antarctica. Nature 219, 476–477.

Droop, G.T.R., 1989. Reaction history of garnet–sapphirine granulites and conditions of Archaean high-pressure granulite-facies metamorphism in the central Limpopo Mobile Belt, Zimbabwe. J. Metamorph. Geol. 7, 383–403.

Droop, G.T.R., Bucher-Nurminen, K., 1984. Reaction textures and metamorphic evolution of sapphirine-bearing granulites from the Gruf Complex, Italian Central Alps. J. Petrol. 25, 766–803.

Enami, M., Zang, Q., 1988. Magnesian staurolite in garnet-corundum rocks and eclogite from the Donghai district, Jiangsu province, east China. Am. Mineral. 73, 48–56.

Fockenberg, T., 1998. An experimental investigation on the P–T stability of Mg-staurolite in the system $MgO–Al_2O_3–SiO_2–H_2O$. Contrib. Mineral. Petrol. 130, 187–198.

Goscombe, B., 1992. Silica-undersaturated sapphirine, spinel and kornerupine granulite facies rocks, NE Strangway Range, Central Australia. J. Metamorph. Geol. 10, 181–201.

Grew, E.S., 1986. Petrogenesis of kornerupine at Waldheim (Sachsen), German Democratic Republic. Z. Geol. Wiss. 14, 525–558.

Guiraud, M., Kienast, J.R., Ouzegane, K., 1996. Corundum–quartz-bearing assemblage in the Ihouhaouene area (in Ouzzal Algeria). J. Metamorph. Geol. 14, 755–761.

Harley, S.L., 1998. On the occurrence and characterization of ultrahigh-temperature crustal metamorphism. Spec. Publ. - Geol. Soc. Lond. 138, 81–107.

Harley, S.L., 2004. Extending our understanding of ultrahigh-temperature crustal metamorphism. J. Mineral. Petrol. Sci. 99, 140–158.

Harlov, D.E., Milke, R., 2002. Stability of corundum+quartz relative to kyanite and sillimanite at high temperature and pressure. Am. Mineral. 87, 424–432.

Harlov, D.E., Milke, R., 2004. Reversal of sillimanite–corundum–quartz: competition between stable and metastable reactions. Lithos 73, S48.

Helgeson, H.C., Delany, J.M., Nesbitt, H.W., Bird, D.K., 1978. Summary and critique of the thermodynamic properties of rock-forming minerals. Am. J. Sci. 278-A, 1–229.

Hellman, P.L., Green, T.H., 1979. The high-pressure experimental crystallization of staurolite in hydrous mafic compositions. Contrib. Mineral. Petrol. 68, 369–372.

Hensen, B.J., Harley, S.L., 1990. Graphical analysis of P–T–X relations in granulite facies metapelites. In: Ashworth, J.R., Brown, M. (Eds.), High-temperature Metamorphism and Crustal Anatexis. Kluwer Academic Publishers, pp. 19–56.

Higgins, J.B., Ribbe, P.H., Herd, R.K., 1979. Sapphirine I: crystal chemical contributions. Contrib. Mineral. Petrol. 68, 349–356.

Hiroi, Y., Ogo, Y., Namba, K., 1994. Evidence for prograde metamorphic evolution of Sri Lankan pelitic granulites, and implications for the development of continental crust. Precambrian Res. 66, 245–263.

Holzer, L., Frey, R., Barton Jr., J.M., Kramers, J.D., 1998. Unravelling the record of successive high-grade events in the Central Zone of the Limpopo Belt using Pb single phase dating of metamorphic minerals. Precambrian Res. 87, 87–115.

Horrocks, P.C., 1983. A corundum and sapphirine paragenesis from the Limpopo Mobile Belt, southern Africa. J. Metamorph. Geol. 1, 13–23.

Jaeckel, P., Kröner, A., Kamo, S.L., Brandl, G., Wendt, J.I., 1997. Late Archaean to early Proterozoic granitoid magmatism and high-grade metamorphism in the central Limpopo Belt, South Africa. J. Geol. Soc. (Lond.) 154, 25–44.

Kamber, B.S., Kramers, J.D., Napier, R., Cliff, R.A., Rollinson, H.R., 1995. The Triangle Shearzone, Zimbabwe, revisited: new data document an important event at 2.0 Ga in the Limpopo Belt. Precambrian Res. 70, 191–213.

Kawasaki, T., 2005. Corundum–quartz coexistence obtained from melting experiments of a pelitic rock. The 25th Symp. Polar Geosci. (Tokyo), Abstr. , pp. 48–49 (in Japanese with English figure captions).

Kawasaki, T., Sato, K., 2002. Experimental study of Fe–Mg exchange reaction between orthopyroxene and sapphirine and its calibration as a geothermometer. Gondwana Res. 5, 741–747.

Koch-Müller, M., 1997. Experimentally determined Fe–Mg exchange between synthetic staurolite and garnet in the system $MgO–FeO–Al_2O_3–SiO_2–H_2O$. Lithos 41, 185–212.

Kornprobst, J., Piboule, M., Roden, M., Tabit, A., 1990. Corundum-bearing garnet clinopyroxenites at Beni-Bousera (Morocco): original plagioclase-rich gabbros recrystallized at depth within the mantle? J. Petrol. 31, 717–745.

Koshimoto, S., Tsunogae, T., Santosh, M., 2004. Sapphirine and corundum bearing ultrahigh temperature rocks from the northern domain of Palghat-Cauvery Shear System, southern India. J. Mineral. Petrol. Sci. 99, 298–310.

Kreissig, K., Holzer, L., Frei, R., Villa, I.M., Kramers, J.D., Kröner, A., Smit, C.A., van Reenen, D.D., 2001. Geochronology of the Hout River Shear Zone and the metamorphism in the Southern Marginal Zone of the Limpopo Belt, southern Africa. Precambrian Res. 109, 145–173.

Krogh, E.J., 1977. Origin and metamorphism of iron formations and associated rocks, Lofoten-Vesterålen, N. Norway: I. The Vestpolltind Fe–Mn deposit. Lithos 10, 243–255.

Kröner, A., Jaeckel, P., Brandl, G., Nemchin, A.A., Pidgeon, R.T., 1999. Single zircon ages for granitoids gneisses in the Central Zone of the Limpopo Belt, southern Africa and geodynamic significance. Precambrian Res. 93, 299–337.

Kretz, R., 1983. Symbols for rock-forming minerals. Am. Mineral. 68, 277–279.

Lal, R.K., Ackermand, D., Upadhyay, H., 1987. P–T–X relationships deduced from corona textures in sapphirine–spinel–quartz assemblages from Paderu, Southern India. J. Petrol. 28, 1139–1168.

McCourt, S., Armstrong, R.A., 1998. SHRIMP U–Pb zircon geochronology of granites from the Central Zone, Limpopo Belt, southern Africa: implications for the age of the Limpopo Orogeny. S. Afr. J. Geol. 101, 329–338.

Motoyoshi, Y., Hensen, B.J., Matsueda, H., 1990. Metastable growth of corundum adjacent to quartz in a spinel-bearing quartzite from the Archean Napier Complex, Antarctica. J. Metamorph. Geol. 8, 125–130.

Mouri, H., Andreoli, M.A.G., Kienast, J.R., Guiraud, M., de Waal, S.A., 2003. First occurrence of the rare 'corundum+quartz' assemblage in the high-grade zone from the Namaqualand Metamorphic Complex, South Africa: evidence of high-*P*, *T* metamorphism? Mineral. Mag. 67, 1015–1021.

Mouri, H., Guiraud, M., Osanai, Y., 2004. Review on "corundum+quartz" assemblage in nature: Possible indicator of ultra-high temperature conditions? J. Mineral. Petrol. Sci. 99, 159–163.

Nichols, G.T., Berry, R.F., Green, D.H., 1992. Internally consistent gahnitic spinel–cordierite–garnet equilibria in the FMASHZn system: geothermobarometry and applications. Contrib. Mineral. Petrol. 111, 362–377.

Osanai, Y., Owada, M., Kawasaki, T., 1992. Tertiary deep crustal ultrametamorphism in the Hidaka metamorphic belt, northern Japan. J. Metamorph. Geol. 10, 401–414.

Peacock, S.M., Goodge, J.W., 1995. Eclogite-facies metamorphism preserved in tectonic blocks from a lower crustal shear zone, central Transantarctic Mountains, Antarctica. Lithos 36, 1–13.

Perchuk, L.L., Lavrent'eva, I.V., 1983. Experimental investigation of exchange equilibria in the system cordierite–garnet–biotite. In: Saxena, S.K. (Ed.), Kinetics and Equilibrium in Mineral Reactions. Springer-Verlag, pp. 199–239.

Perchuk, L., Gerya, T., Nozhkin, A., 1989. Petrology and retrograde P–T path in granulites of the Kanskaya formation, Yenisey range, Eastern Siberia. J. Metamorph. Geol. 7, 599–617.

Perchuk, L.L., Gerya, T.V., van Reenen, D.D., Krotov, A.V., Safonov, O.G., Smit, C.A., Shur, M.Yu., 2000. Comparative petrology and metamorphic evolution of the Limpopo (South Africa) and Lapland (Fennoscandia) high-grade terrains. Mineral. Petrol. 69, 69–107.

Powers, R.E., Bohlen, S.R., 1985. The role of synmetamorphic igneous rocks in the metamorphism and partial melting of metasediments, Northwest Adirondacks. Contrib. Mineral. Petrol. 90, 401–409.

Roering, C., van Reenen, D.D., Smit, C.A., Barton Jr., J.M., de Beer, J.H., de Wit, M.J., Stettler, E.H., van Schalkwyk, J.F., Stevens, G., Pretorius, S., 1992. Tectonic model for the evolution of the Limpopo Belt. Precambrian Res. 55, 539–552.

Rollinson, H.R., Blenkinsop, T., 1995. The magmatic, metamorphic and tectonic evolution of the Northern Marginal Zone of the Limpopo Belt in Zimbabwe. J. Geol. Soc. (Lond.) 152, 65–75.

Schreyer, W., 1988. Experimental studies on metamorphism of crustal rocks under mantle pressures. Mineral. Mag. 52, 1–26.

Schreyer, W., Horrocks, P.C., Abraham, K., 1984. High-magnesium staurolite in a sapphirine–garnet rock from the Limpopo Belt, southern Africa. Contrib. Mineral. Petrol. 86, 200–207.

Shaw, R.K., Arima, M., 1998. A corundum–quartz assemblage from the Eastern Ghats Granulite Belt, India: evidence for high P–T metamorphism? J. Metamorph. Geol. 16, 189–196.

Shimpo, M., Tsunogae, T., Santosh, M., 2006. First report of garnet–corundum rocks from southern India: implications for prograde high-pressure (eclogite-facies?) metamorphism. Earth Planet. Sci. Lett. 242, 111–129.

Spear, F.S., Cheney, J.T., 1989. A petrogenetic grid for pelitic schists in the system SiO_2–Al_2O_3–FeO–MgO–K_2O–H_2O. Contrib. Mineral. Petrol. 101, 149–164.

Tsunogae, T., Miyano, T., 1989. Granulite facies metamorphism in the Central and Southern Marginal Zones of the Limpopo Belt, South Africa. J. Geol. Soc. Japan 95, 1–16 (in Japanese with English abstr.).

van Reenen, D.D., Barton Jr., J.M., Roering, C., Smit, C.A., van Schalkwyk, J.F., 1987. Deep crustal response to continental collision: the Limpopo Belt of southern Africa. Geology 15, 11–14.

van Reenen, D.D., Roering, C., Brandl, G., Smit, C.A., Barton Jr., J.M., 1990. The granulite-facies rocks of the Limpopo Belt, southern Africa. In: Vielzeuf, D., Vidal, Ph. (Eds.), Granulites and Crustal Evolution. Kluwer, Dordrecht, pp. 257–289.

van Reenen, D.D., Perchuk, L.L., Smit, C.A., Varlamov, D.A., Boshoff, R., Huizenga, J.M., Gerya, T.V., 2004. Structural and P–T evolution of a major cross fold in the Central Zone of the Limpopo high-grade terrain, South Africa. J. Petrol. 45, 1413–1439.

Windley, B.F., Ackermand, D., Herd, R.K., 1984. Sapphirine/kornerupine-bearing rocks and crustal uplift history of the Limpopo Belt, southern Africa. Contrib. Mineral. Petrol. 86, 342–358.

Zeh, A., Klemd, R., Buhlmann, S., Barton Jr., J.M., 2004. Pro- and retrograde PT evolution of granulites of the Beit Bridge Complex (Limpopo Belt, South Africa): constraints from quantitative phase diagrams and geotectonic implications. J. Metamorph. Geol. 22, 79–95.

Zhang, R.Y., Liou, J.G., Zheng, J.P., 2004. Ultrahigh-pressure corundum-rich garnetite in garnet peridotite, Sulu terrane, China. Contrib. Mineral. Petrol. 147, 21–31.